



Properties of the avalanche photodiodes for the CMS electromagnetic calorimeter

K. Deiters^{a,*}, Q. Ingram^a, Y. Musienko^{c,1}, S. Nicol^c, P. Patel^b, D. Renker^a,
S. Reucroft^c, R. Rusack^b, T. Sakhelashvili^a, J. Swain^c, P. Vikas^b

^aPaul Scherrer Institut, CH-5232 Villigen-PSI, Switzerland

^bUniversity of Minnesota, Minneapolis, USA

^cNortheastern University, Boston, USA

Accepted 19 June 2000

Abstract

The electromagnetic calorimeter of the CMS experiment at CERN's Large Hadron Collider will use 122400 Avalanche Photodiodes from Hamamatsu Photonics. The design of this APD type is the result of a long R&D program performed by Hamamatsu Photonics and the CMS collaboration. The APD parameters including the behavior under irradiation are discussed in view of our application. © 2000 Elsevier Science B.V. All rights reserved.

1. Introduction

The barrel of the electromagnetic calorimeter of the CMS detector will be made out of 61 200 lead tungstate crystals. The design of the CMS detector and the operating conditions of the LHC require that the photosensors operate in a magnetic field of 4 T and can withstand high radiation levels. In addition, since the crystals have a relatively low light yield, the photosensors need to have a comparably small electrical response to ionizing particles passing through them (low nuclear counter effect). In 1993, initial beam tests with a prototype APD from Hamamatsu Photonics and a PbWO₄ crystal showed that Avalanche Photodiodes

(APDs) could be used with these crystals but some operating parameters (see Table 1) required considerable improvement. We launched an R&D program with Hamamatsu Photonics and with EG&G Opto-Electronique to develop a suitable APD for the CMS electromagnetic calorimeter. In 1998, this effort was concentrated at Hamamatsu Photonics who are now producing APDs which are well suited for this application.

2. Properties of APDs

The Hamamatsu APDs are made by epitaxial growth on low resistivity n⁺-type silicon followed by ion implantation and diffusion steps. The basic structure of the APD is shown in Fig. 1. The pn-junction depth is set at around 5 μm to minimize the sensitivity to ionizing radiation and to maximize the absorption of the blue light from the

*Corresponding author. Tel.: +41-56310-4241; fax: +41-56310-3294.

¹On leave from INR (Moscow).

Table 1
Parameters of recent APDs in comparison to a 1993 prototype

Parameter	1999	1993
Active area	$5 \times 5 \text{ mm}^2$	$\emptyset 5 \text{ mm}$
Op. voltage	$\sim 380 \text{ V}$	
Capacitance	70 pF	320 pF
Serial resist.	3Ω	
Dark current	$< 10 \text{ nA}$	800 nA
Quantum eff.	72% for 420 nm	
$dM/dV \times 1/M$	3%/V	15%/V
$dM/dT \times 1/M$	$-2.2\%/^{\circ}\text{C}$	

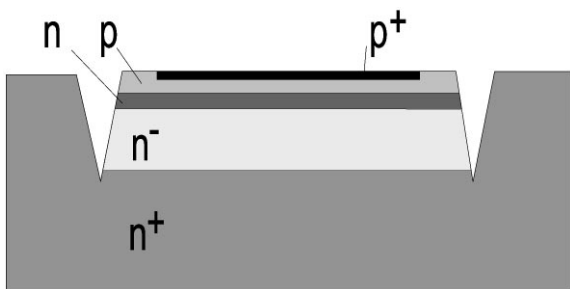


Fig. 1. APD structure.

crystal. The n^- layer was introduced to increase the thickness of the depletion region. This decreased both the capacitance and the sensitivity of the gain to changes in the applied bias. The $30 \mu\text{m}$ deep V-shaped grooves around the cathode were found to be necessary to reduce surface currents, especially important after the APD has received a large radiation dose.

2.1. The nuclear counter effect

Ionizing particles passing through the crystals generate electron–hole pairs in the APD. Electrons generated in front of the pn-junction and holes generated behind the junction will drift through the avalanche region. Since electrons have a much higher probability of initiating an avalanche than holes, only the electrons generated in the p-region will produce significant electrical signals. Conversely, blue light is absorbed almost entirely in the p-region. Thus, the signal is maximally amplified while the signal from ionizing particles is suppressed. One measure of this effect is to compare

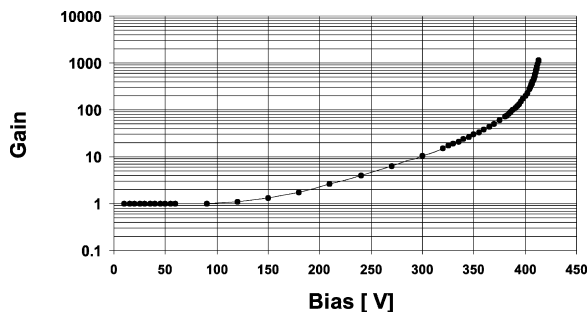


Fig. 2. Gain vs. bias voltage. The gain is 50 at about 370 V.

the signal from a minimum-ionizing particle crossing a PIN diode without any multiplication with the signal from an APD divided by the gain. By comparing the output of the APD when an electron crosses it we find that the equivalent APD thickness is $5.6 \mu\text{m}$ [1], compared to figure of $200 \mu\text{m}$ which would be obtained with a standard PIN diode.

2.2. Gain-and-gain stability

Fig. 2 shows how the APD gain changes with the applied bias voltage. For these measurements a blue LED, with peak output at 430 nm, illuminates the APD. For bias voltages less than 50 V [2] the APDs have unity gain and here the signal at 20 V is used to normalize the gain at higher voltages. The change of gain with bias voltage when the gain is 50, the nominal operating value is shown in Fig. 3 and is given by

$$dM/dV \times 1/M = 3.0\%/V. \quad (1)$$

Since the avalanche multiplication depends on the mean free path of electrons between ionizing collisions, which is temperature dependent, the APD gain varies with temperature (Fig. 4). This variation can be described by the relationship

$$dM/dT \times 1/M = -2.2\%/^{\circ}\text{C}. \quad (2)$$

2.3. Excess noise factor

In avalanche multiplication only one secondary is generated per collision, leading to larger gain

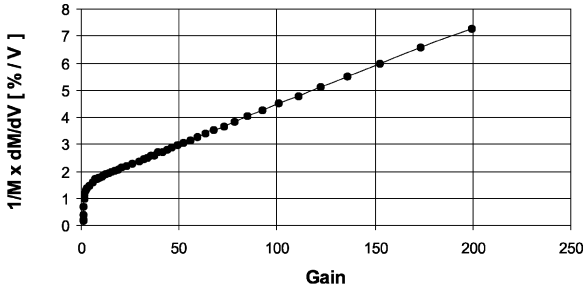


Fig. 3. Change of gain with the bias voltage.

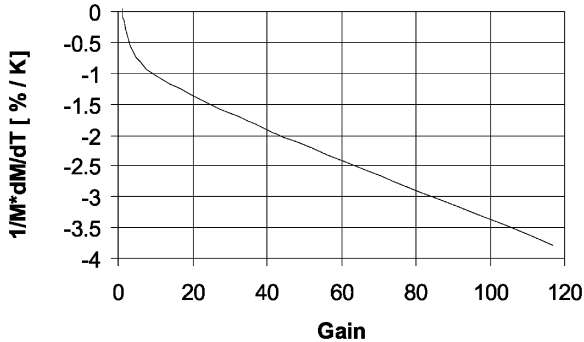


Fig. 4. Change of gain with the operation temperature.

fluctuations than observed in conventional photo-multiplier tubes. Another fluctuation is caused by the contribution of holes to the gain. These effects contribute to the excess noise factor of the amplification process. For high gain (≥ 50), F can be approximated with the following equation [3]:

$$F = k \times M \times (2 - 1/M) \times (1 - k) \quad (3)$$

where k is the ratio of the ionization coefficients for holes and electrons and M is the APD gain. At a gain of 50, the APDs have an excess noise factor of 2 (Fig. 5).

2.4. Radiation hardness

To test the radiation hardness of the APDs, they were irradiated for about 2 h with a 2 nA beam of 64 MeV protons. This dose corresponds to a neutron flux of about 2×10^{13} neutrons/cm² [4], the expected total neutron fluence after 10 years of LHC operation in the central section of the calorimeter.

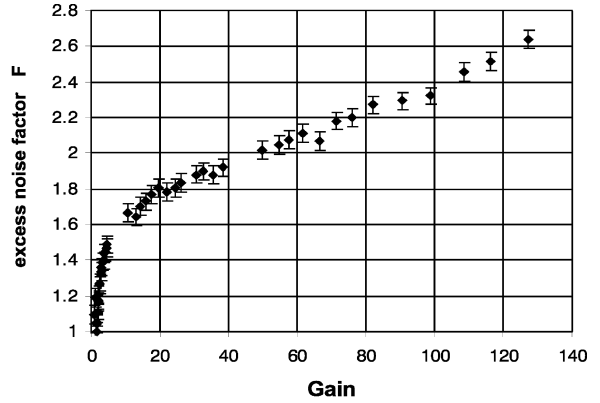


Fig. 5. Excess noise factor F vs. gain.

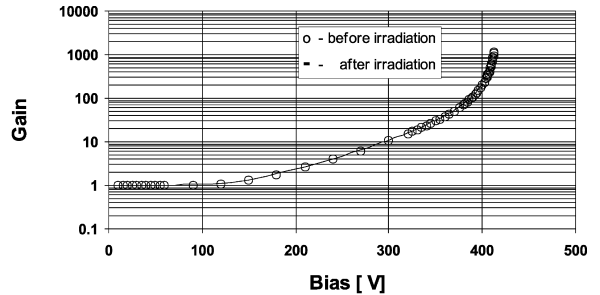


Fig. 6. Gain vs. bias voltage before and after an irradiation with protons.

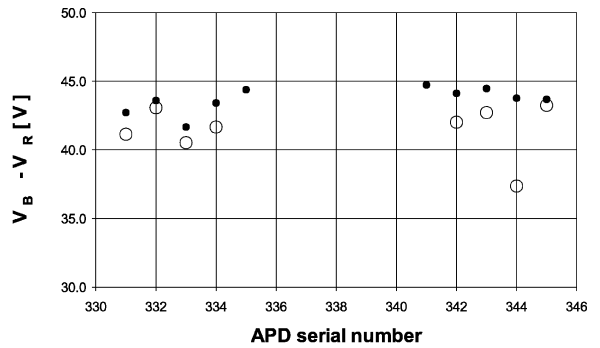


Fig. 7. Distance of bias voltage for a gain of 50 to breakdown voltage for an APD before (dots) and after irradiation (circles).

During the irradiation the APDs are operated at a gain of 50.

Afterwards they were annealed for a week at a temperature of 90°C and all parameters were re-measured. In Fig. 6 measurements taken before

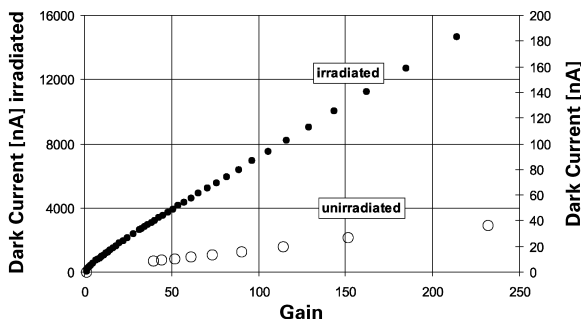


Fig. 8. Dark current vs. gain for an APD before and after irradiation.

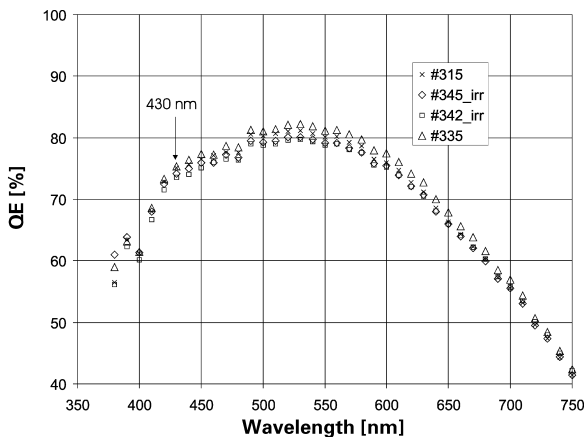


Fig. 9. Quantum efficiency vs. wavelength for two unirradiated and two irradiated APDs.

and after irradiation of the gain are compared and it can be seen that the bias voltage needed for a gain of 50 changes only by 1 V.

For the safe operation of an APD, the difference between the operating voltage at gain 50 and the

breakdown voltage is important. Fig. 7 shows this difference for unirradiated APDs and for the same APDs after irradiation. The mean difference changes only slightly from 44 to 42 V. The dark current at gain 50 increases from 10 nA before irradiation to about 4 μ A after irradiation and annealing (Fig. 8) at an operation temperature of 25°C.² All other parameters: the capacitance, series resistance, dM/dV , dM/dT and the quantum efficiency at gain 50 (see Fig. 9) do not change during irradiation.

3. Summary

Table 1 summarizes the parameters of the APDs. Compared to the 1993 prototype the state-of-the-art APDs for crystal calorimeters has been greatly improved. Now in situ irradiation causes only a rise of the dark current while other parameters are stable. In the CMS detector the gain variation of 3%/V will require a good-quality bias supply, but the demonstrated stability of the other APD parameters will help to keep the contribution from the APD to the constant term in the calorimeter energy resolution small compared to the goal of 0.5% after 10 years of LHC operation.

References

- [1] D. Renker, Nucl. Instr. and Meth. (2000), submitted for publication.
- [2] A. Karar et al., Nucl. Instr. and Meth. A 428 (1999) 413.
- [3] R. McIntyre, IEEE Trans. Electron Dev. ED-19 (1972) 703.
- [4] M. Huhtinen, P. Aarnio, Nucl. Instr. and Meth. A 335 (1993) 580.

² The ECAL operation temperature will be 18°C where the dark current will be a factor of two less, around 2 μ A.